TAC: THRESHOLDING ACTIVE CONTOURS

Samuel Dambreville, Anthony Yezzi, Shawn Lankton and Allen Tannenbaum

School of Electrical and Computer Engineering
Georgia Institute of Technology
Atlanta, GA 30332-0250

ABSTRACT

In this paper, we describe a region-based active contour technique to perform image segmentation. We propose an energy functional that realizes an explicit trade-off between the (current) image segmentation obtained from a curve and the (implied) segmentation obtained from *dynamically* thresholding the image. In contrast with standard region-based techniques, the resulting variational approach bypasses the need to fit (*a priori* chosen) statistical models to the object and the background. Our technique performs segmentation based on geometric considerations of the image and contour, instead of statistical ones. The resulting flow leads to very reasonable segmentations as shown by several illustrative examples.

Index Terms— Variational methods, geometric active contours, thresholding, level sets, partial differential equations.

1. MOTIVATION AND RELATED WORK

Segmentation involves separating an image into distinct regions, a ubiquitous task in computer vision applications. The active contour technique has been proven to be a very valuable tool for performing this task [1, 2, 3, 4].

Relation to prior work: In the geometric active contour (GAC) framework, a closed curve is represented implicitly as the zero level-set of a higher dimensional function, usually a signed distance function [5]. The implicit representation allows the curve to naturally undergo topological changes, such as splitting and merging. Different models have been proposed to perform segmentation with GACs: Some frameworks use local image features such as edges [6, 7], whereas other methods use regional image information such as intensity statistics, color or texture [8, 1, 9, 10]. Region-based approaches usually yield more robust performances than techniques based on local information. Many of the region-based models have been inspired by the region competition technique proposed in [11].

In region-based frameworks, intensity statistics are usually estimated from the segmenting curve using parametric [1, 8, 10] or non-parametric [9] methods. Most of the region-based techniques previously proposed measure discrepancies between the statistics of the pixels located inside and outside the segmenting curve.

Motivation: However, segmentation can be regarded as the problem of finding a certain shape in an image and the statistics of pixels

intensities are only a means to this end. Based upon this observation, we propose a novel region-based segmentation technique using GACs. We present a variational formulation, in which we minimize an energy functional that compares two shapes: The shape of the segmenting contour and a shape extracted from the image via a **dynamic** thresholding operation. Our methodology does not require one to fit *a priori* chosen statistical models of regions.

This paper is organized as follows: In the next section, we describe the proposed approach, the novel energy functional and flow. We then present experimental results that highlight the specificities of the novel approach as well as its improved performance over standard techniques, on challenging artificial and real images. Finally, we summarize our work and make some conclusions.

2. PROPOSED APPROACH

2.1. Notation and Problem Formulation

We consider the problem of segmenting an image $I : \Omega \mapsto \mathcal{Z}$, where $\Omega \subset \mathbb{R}^2$ is the image domain and $\mathcal{Z} \subset \mathbb{R}^n$ is the space of pixel intensity values. The area element of Ω will be denoted $d\Omega$ and $x \in \Omega$ will specify the coordinates of the pixels in the image I. We assume that I is composed of two (unknown) regions, referred to as "Object" and "Background." The goal of segmentation is to capture these two regions.

To do so, we evolve a closed curve C, represented as the zero level-set of a signed distance function $\phi : \Omega \mapsto \mathbb{R}$, such that $\phi > 0$ inside C and $\phi < 0$ outside C. Our goal is to evolve the contour C (through ϕ) so that its interior matches the Object, and its exterior matches the Background: the curve C would then match the boundary $\partial \Omega$ separating Object and Background. The region inside C (respectively, outside) will be denoted R (respectively $R^c = \Omega \setminus R$).

Let us denote by $H : \mathbb{R} \mapsto \{0, 1\}$ the Heaviside step function,

$$H(\chi) = \begin{cases} 1 & \text{if } \chi \geq 0; \\ 0 & \text{if } \chi < 0. \end{cases}$$

The derivative of H is given by $\delta(\chi) = \delta\chi = \frac{dH}{d\chi}$.

In this paper, a shape $\mathcal{S} \subset \Omega$ is characterized by a characteristic function $S_{\mathcal{S}} : \Omega \mapsto \{0, 1\}$ such as

$$S_{\mathcal{S}}(x) \begin{cases} = 1 & \text{if } x \in \mathcal{S}; \\ = 0 & \text{if } x \in \Omega \setminus \mathcal{S}. \end{cases}$$

The function H described above can be used as a characteristic function to describe shapes. For instance, the shape defined by the interior of the contour C can be characterized by the characteristic function $H\phi$.

Let $G(\tau, I(x)) = 1$ or 0 denote the result of thresholding the image using the threshold(s) $\tau = (\tau_1, ..., \tau_N)$ and with the convention that pixels such that $G(\tau, I(x)) = 1$ correspond to pixels deemed to belong to the Object (see e.g., [12, 13], for more details about image thresholding). From the definition of shape above, the functional G can be interpreted as a shape extracted from the image.

2.2. Energy Functional

In most of the region-based segmentation techniques, the assumption is made that the Object and Background are characterized by certain statistical properties, which are visually consistent and distinct from each other. From this hypothesis, most of the region-based techniques that do not assume prior knowledge of intensity distributions, work directly with the densities P_{in} and P_{out} (the conditional distributions of the pixels inside and outside the curve, respectively) to increase their difference in the hope of converging towards the "true" densities P_{O} and P_{B} (the distributions of the pixels belonging to the Object and the Background, respectively). Typically, an energy functional that measures the similarity between P_{in} and P_{out} (or simply statistical moments) is defined and minimized. Thus, the differences among approaches mainly resides in the choice of the measure of similarity among intensity statistics or densities.

In this work, we propose to minimize the following energy in order to perform the segmentation:

$$
\begin{aligned}
E_{\mathrm{im}}(C, \tau) &= \|H\phi(C) - G(C)\|^2 \\
&= \int_\Omega \big(H\phi(x) - G(\tau, I(x))\big)^2 d\Omega \\
&= \int_{\mathrm{R}} \big(1 - G(\tau, I(x))\big) d\Omega + \int_{\mathrm{R^c}} G(\tau, I(x)) \, d\Omega
\end{aligned}
$$
$$(1)$$

In contrast with standard region-based approaches, this energy does not necessarily involve pixel statistics inside and outside the curve. Minimizing such an energy can be beneficial when statistical models cannot properly distinguish between regions of interest. Furthermore, one can note that regions in two given images can have very similar statistics but represent very different objects. As a result, the segmentation task can be regarded as the problem of finding a certain shape in an image, and the statistics of pixels intensities are only one possible means to this end. Thus, focusing on statistics alone may not be sufficient.

As can be noted from Equation (1), the energy E_{im} is the L_2 distance between two shapes: the shape of the region defined by the interior of the curve C and the shape G extracted from the image. This is in accordance with the intuition that segmentation is about extracting shapes, the functional G has been formulated in a natural manner for learning the shape of the object of interest online. Furthermore, minimizing E_{im} effectively amounts to realizing a trade-off between the segmentation obtained from the curve C and the segmentation obtained from thresholding the image. (The thresholding operation is taken *as a function of the curve C* in this work. In particular, G varies when C varies).

This set-up allows us to take advantage of the flexibility of the thresholding technique, see for example [13], while ameliorating some of its typical weaknesses such as lack of locality (thresholding is a global operation, and supervision is usually required to choose parts of interest in the thresholded image). Here, the locality of the active contour is exploited. Also, meaningful geometric constraints can be imposed to the curve C to improve segmentation results. For instance, the smoothness of the results can be controlled by using a

curvature term (such regularization is difficult to impose on thresholding: approaches)

$$
E_T(C, \tau) = E_{\mathrm{im}}(C, \tau) + \int_C ds. \tag{2}
$$

In what follows, we study the flows that are obtained when the function G is constructed by using optimal thresholds for E_{im}. This allows the exploitation of geometric information in the image, without necessitating one to fit statistical models to the image data.

2.3. Gradient Flow

In Equation (1), the unknowns are the curve C and the threshold(s) τ. We now present the details of the flow obtained when one solves optimally for both C^* and τ^* for gray-scale images in which $\mathcal{Z}$ is a closed interval of positive real numbers. (The general case for vector valued images will be detailed elsewhere.) In this case, one has a joint minimization problem of the form

$$
(C^*, \tau^*) = \arg\min_{C, \tau} \left(E_{\mathrm{im}}(C, \tau)\right). \tag{3}
$$

Hence, when optimal threshold(s) are computed, the energy E_{im} compares the two shapes $H\phi$ and G based only on geometric considerations: it is minimal when the *graphs* of the label maps $H\phi$ and G coincide in a maximal fashion over the entire domain Ω.

2.3.1. Thresholding with one threshold

The elementary way of thresholding the gray-scale image I with the threshold τ is to compute

$$
G(\tau, x) = H\big(I(x) - \tau\big) \tag{4}
$$

when the object of interest is lighter than the background, or

$$
G(\tau, x) = 1 - H\big(I(x) - \tau\big) = H\big(-(I(x) - \tau)\big) \tag{5}
$$

when the object of interest is darker than the background.

For the definition of G in Equation (4), one can compute $E'_{\mathrm{im}}(\tau) = \frac{\partial E_{\mathrm{im}}}{\partial \tau}$ from Equation (1)

$$
\frac{\partial E_{\mathrm{im}}}{\partial \tau} = \int_R \delta\big(I(x) - \tau\big) - \int_{R^c} \delta\big(I(x) - \tau\big). \tag{6}
$$

Using the scaling property of the Dirac delta function generalized to multidimensional functionals (co-area formula), one gets

$$
\frac{\partial E_{\mathrm{im}}}{\partial \tau} = \int_{\Gamma \,\cap\, \mathrm{R}} \frac{ds'}{\|\nabla_x I\|} - \int_{\Gamma \,\cap\, \mathrm{R^c}} \frac{ds'}{\|\nabla_x I\|} \tag{7}
$$

where $\nabla_x I$ denotes the gradient of the image with respect to the spatial (Euclidean) coordinates, and the curve Γ, parameterized with arclength s', represents the isolines in I such that $I = \tau$, i.e.:

$$
\Gamma = \{x \in \Omega \quad \text{s.t.} \quad I(x) = \tau\}
$$

Hence, the curve $\Gamma = \partial G$ corresponds to the edges of the thresholded image G. One notes that Equations (6) and (7) are defined if and only if $\nabla_x I \neq 0$ on Γ. This condition can be easily enforced on quantized images, as described in the sequel.

Considering the function $E'_{\mathrm{im}}(\tau)$ in Equations (6) or (7), one can compute the *optimal* threshold $\tau^*(C)$ for the energy E_{im}, given the curve C. This optimal threshold is such that $\frac{\partial E_{\mathrm{im}}}{\partial \tau}(\tau^*(C)) = 0$, $\frac{\partial E_{\mathrm{im}}}{\partial \tau}(\tau^{*+}(C)) > 0$, and $\frac{\partial E_{\mathrm{im}}}{\partial \tau}(\tau^{*-}(C)) < 0$.

746

Once the threshold $\tau^*(C)$ is computed, the energy E_{im} can be minimized with respect to C using gradient descent, with

$$\nabla_C E_{\text{im}}(x) = \left(1 - 2G(\tau^*(C), x)\right).\mathbf{N}(x) \tag{8}$$

where $\mathbf{N}(\mathbf{x})$ is the outward normal to the curve at the point x. The flow minimizing the Energy E_T, is then

$$\frac{dC}{dt} = -\left(1 - 2G\right).\mathbf{N} - \kappa.\mathbf{N} \tag{9}$$

where $\kappa(x)$ is the curvature of the curve C at x.

One then iterates the process described above, alternating between the computation of $\tau^*(C)$ and the evolution of C, until the convergence of both $\tau^*(C)$ and C to τ^* and C^*, respectively.

In practice, and from an initial guess $\tau_{t=0}^*{}^1$ for τ^*, one can detect changes in the sign of $E'_{\text{im}}(\tau) = \frac{\partial E_{\text{im}}}{\partial \tau}$, for quantized values of the thresholds τ (i.e., values of $\tau \in \mathcal{Z}_{\frac{1}{2}} = \{-0.5, 0.5, 1.5, ...254.5\}$). Let τ_a and $\tau_b = \tau_a + 1$ be the threshold values, closest to $\tau_{t=0}^*$, such that $E'_{\text{im}}(\tau)$ changes sign. One can then choose $\tau^*(C)$ to be the threshold between τ_a and τ_b that leads to the lowest energy E_{im}.

$$\tau^*(C) = \arg \min_{\tau_a, \tau_b} E_{\text{im}}(C, \tau) \tag{10}$$

N.B. 1: The computations of τ_a, τ_b and $\tau^*(C)$ above are valid for G computed using Equation (4). However, one can note that the expression of $E'_{\text{im}}(\tau)$ simply changes sign when G is computed using Equation (5). Hence, one can *first* perform the computations of τ_a, τ_b and $\tau^*(C)$ using the expression of $E'_{\text{im}}(\tau)$ in Equation (6), and *then* compute G using Equation (4) if $E'_{\text{im}}(\tau_a) < 0$ and $E'_{\text{im}}(\tau_b) > 0$ or using Equation (5) if $E'_{\text{im}}(\tau_a) > 0$ and $E'_{\text{im}}(\tau_b) < 0$.

N.B. 2: The derivative $E'_{\text{im}}(\tau)$ is well defined, for the thresholds $\tau \in \mathcal{Z}_{\frac{1}{2}}$ since $I(x) \in \mathcal{Z}$ and, thus, necessarily $\nabla_x I \neq 0$, $\forall x \in \Gamma$

2.3.2. Thresholding with multiple thresholds

Thresholding the gray-scale image I with multiple thresholds $\tau = (\tau_1, \ldots, \tau_N)$ may be undertaken by computing

$$G(\tau, x) = H\left(\pm \prod_{i=1}^{N} \left(I(x) - \tau_i\right)\right) = H\left(\mathcal{T}_m(x, \tau)\right). \tag{11}$$

We compute the derivative of E_{im} with respect to a particular threshold τ_{i0}:

$$\frac{dE_{\text{im}}}{d\tau_{i0}} = \int_R \delta\left(\mathcal{T}_m(x, \tau)\right) \left(\pm \prod_{i \neq i0} \left(I(x) - \tau_i\right)\right) d\Omega$$
$$- \int_{R^c} \delta\left(\mathcal{T}_m(x, \tau)\right) \left(\pm \prod_{i \neq i0} \left(I(x) - \tau_i\right)\right) d\Omega \tag{12}$$

Similar to preceding section, we define the curve Γ_{i0}, parameterized with arclength s' as

$$\Gamma_{i0} = \{x \in \Omega \quad \text{s.t.} \quad I(x) = \tau_{i0}\}.$$

Also, one can compute the gradient of $\mathcal{T}_m$ with respect to spatial coordinates as

$$\nabla_x \mathcal{T}_m = \pm \sum_{k=1}^{N} \left(\prod_{i \neq k} \left(I(x) - \tau_i\right)\right) \nabla_x I. \tag{13}$$

---

^{1}Typically one can take the average of the mean intensities inside and outside C for $\tau_{t=0}^*$, at the very first step of the contour evolution. For successive steps, the value $\tau_{t=0}^*$ is taken to the value τ^* found in the preceding step.

For $x \in \Gamma_{i0}$, one has

$$\nabla_x \mathcal{T}_m(x) = \pm \prod_{i \neq i0} \left(\tau_{i0} - \tau_i\right) \nabla_x I. \tag{14}$$

Assuming again that $\nabla_x I \neq 0$ and using the scaling property of the Dirac delta function, one gets

$$\frac{dE_{\text{im}}}{d\tau_{i0}} = \text{sign}\left(\pm \prod_{i \neq i0} \left(\tau_{i0} - \tau_i\right)\right) \times$$
$$\left\{\int_{R \cap \Gamma_{i0}} \frac{ds'}{\|\nabla_x I\|} - \int_{R^c \cap \Gamma_{i0}} \frac{ds'}{\|\nabla_x I\|}\right\} \tag{15}$$

Considering the function

$$\beta(\tau_{i0}, C) = \left\{\int_{R \cap \Gamma_{i0}} \frac{ds'}{\|\nabla_x I\|} - \int_{R^c \cap \Gamma_{i0}} \frac{ds'}{\|\nabla_x I\|}\right\}$$

of the variable τ_{i0} (for a given curve C), one can detect the values of τ_{i0} for which the derivative $\frac{dE_{\text{im}}}{d\tau_{i0}}(\tau_{i0}) = 0$. In practice, this can be done similarly as in the section above by detecting the sign changes of $\beta(\tau_{i0})$, for quantized values of the thresholds τ_{i0} (e.g., values of $\tau_{i0} \in \mathcal{Z}_{\frac{1}{2}}$). Let N be the number of sign changes detected. Let $\tau_{a,j}$ and $\tau_{b,j} = \tau_{a,j} + 1$ (for $j \in [1, N]$) be quantized values such that $\beta(\tau_{i0})$ changes sign (i.e., $\beta(\tau_{a,j})\beta(\tau_{b,j}) < 0$). For each $1 \leq j \leq N$, one defines

$$\tau_j^*(C) = \arg \min_{\tau_{i0} = \tau_{a,j}, \tau_{b,j}} \left(|\beta(\tau_{i0})|\right). \tag{16}$$

One can compute the thresholded image $G^*(C)$, using $\tau = \tau^*(C) = (\tau_1^*(C), \ldots, \tau_N^*(C))$ in Equation (11) (Choosing the sign of the argument of the Heaviside function that leads to the minimum of the energy E_{im}.) This thresholded image $G^*(C)$ is the *optimal thresholded image* corresponding to the *global* minimum of E_{im}, given C (this can be proven studying the function $E_{\text{im}}(\tau_{i0})$ and using the definition of the thresholds $\tau_j^*(C)$).

N.B.3: The procedure described above to compute G^* allows us not only to compute the optimal thresholds $\tau_j^*(C)$, but also their number N. Knowing the number of thresholds to use *a priori* is a challenging problem for most standard thresholding techniques. Here, the information embedded in the shape of the curve C is used to determine the optimal number of thresholds. This is an interesting and valuable feature of the proposed method.

3. EXPERIMENTS

We now present some experiments that illustrate the performance of the proposed framework that uses geometric information only.

Figure 1 presents comparative segmentation results on a synthetic image and a magnetic resonance (MR) image of a heart. Our method was applied on both images using a single threshold as presented in Section 2.3.1. Note that the word "Yellow" is accurately segmented using our technique in the artificial image. Also, the left ventricle is accurately segmented in the MR image. One can compare to the results obtained when two purely statistical methods, as presented in [1] and [10], are run on the same two images for identical initializations. The two methods fit Gaussian models to the regions inside and outside the curve to perform segmentation. For both images, the two statistical methods fail to lead to satisfying segmentations, and end up capturing much bigger regions than the regions
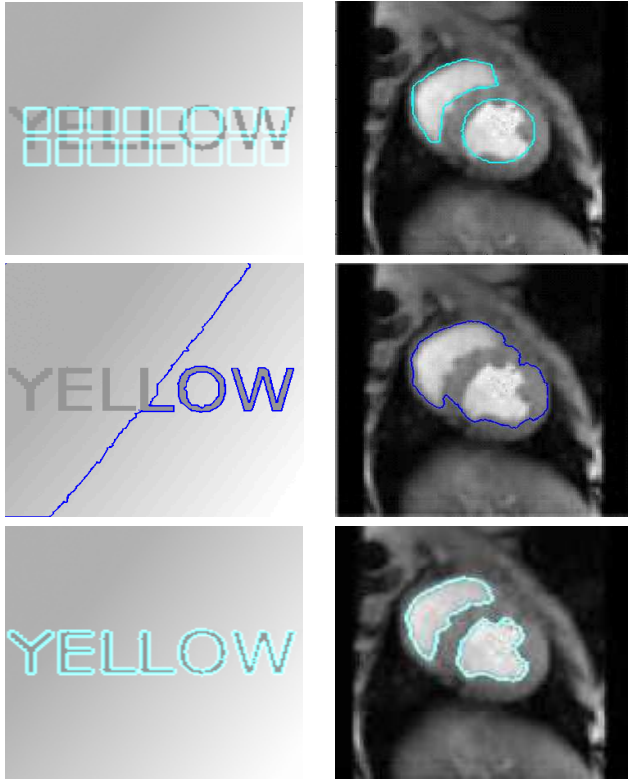
Fig. 2. Segmentation of an image with complex illumination, using multiple optimal thresholds. *Left:* Initialization - 6 optimal thresholds used; *Right:* Result - 5 thresholds used.

Fig. 1. Segmentation of an artificial and an MR image. *Top row:* Initializations; *Middle row:* Typical result with the methods in [1] or [10]; *Bottom row:* Result with the proposed method, using a unique *optimal* threshold.

of interest (even if the contours are initialized very close to the ventricles). These two images are typical cases where statistical models do not properly distinguish between regions of interest and where our proposed geometric approach leads to superior results.

In Figure 2, an image of a toy monkey under complex lighting conditions is successfully segmented by the proposed method using multiple thresholds. At initialization, 6 optimal thresholds are found, whereas 5 thresholds are determined later on during the evolution.

4. CONCLUSIONS

In this work, we presented a novel region-based approach that performs segmentation using geometric information in images. No statistical model needs to be fit to the regions inside and outside the segmenting curve. This can be beneficial when statistical models cannot describe regions in a satisfying manner. In addition, our approach requires less supervision than the standard region-based paradigm since no choice needs to be made on the part of the operator concerning which statistical model to use to perform segmentation.

Our approach has a strong shape interpretation and is based on *dynamically* computing the best thresholded image *as a function of the segmenting curve* at each step of the contour evolution. The thresholding operation can be undertaken using a single or multiple threshold(s). The *number* of optimal thresholds can also be computed automatically. Finally, the proposed methodology performed quite well compared with standard region-based techniques on chal-
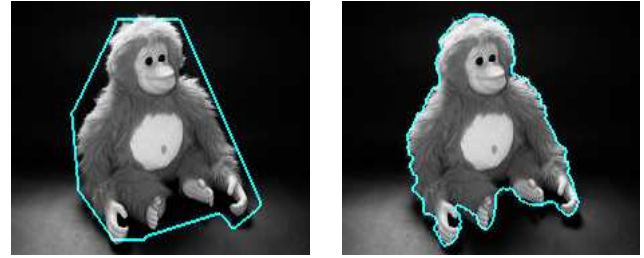
lenging artificial and real-world images.

5. REFERENCES

[1] T. Chan and L. Vese, "Active contours without edges," *IEEE Trans. on Image Processing*, vol. 10, no. 2, pp. 266–277, 2001.

[2] D. Cremers, T. Kohlberger, and C. Schnoerr, "Shape statistics in kernel space for variational image segmentation," in *Pattern Recognition*, 2003, vol. 36, pp. 1292–1943.

[3] M. Kass, A. Witkin, and D. Terzopoulos, "Snakes: active contour models," *IJCV*, vol. 1, pp. 321–331, 1987.

[4] T. Zhang and D. Freedman, "Tracking objects using density matching and shape priors," in *Proc. of the Ninth Int. Conf. on Computer Vision*. IEEE, 2003, pp. 1950–1954.

[5] J. A. Sethian, *Level Set Methods and Fast Marching Methods*, 1999.

[6] V. Caselles, R. Kimmel, and G. Sapiro, "Geodesic active contours," in *IJCV*, 1997, vol. 22, pp. 61–79.

[7] S. Kichenassamy, S. Kumar, P. Olver, A. Tannenbaum, and A. Yezzi, "Conformal curvature flow: From phase transitions to active vision," in *Archives for Rational Mechanics and Analysis*, 1996, vol. 134, pp. 275–301.

[8] A. Yezzi, A. Tsai, and A. Willsky, "A statistical approach to snakes for bimodal and trimodal imagery," in *Proc. ICCV*, 1999, vol. 2, pp. 898–903.

[9] J. Kim, J. Fisher, A. Yezzi, M. Cetin, and A. Willsky, "Nonparametric methods for image segmentation using information theory and curve evolution," in *Proc. ICIP*, 2002, vol. 3, pp. 797–800.

[10] M. Rousson and R. Deriche, "A variational framework for active and adaptative segmentation of vector valued images," in *Proc. Workshop on Motion and Video Computing*, 2002, p. 56.

[11] S. Zhu and A. Yuille, "Region competition: Unifying snakes, region growing, and Bayes/MDL for multiband image segmentation," *IEEE Trans. PAMI*, vol. 18, no. 9, pp. 884–900, 1996.

[12] R. C. Gonzalez and R. E. Woods, *Digital Image Processing*, Addison-Wesley Longman., 2001.

[13] M. Sezgin and B. Sankur, "Survey over image thresholding techniques ad quantitaive performance evaluation," *Journal of Electronic Imaging*, vol. 13, no. 1, pp. 146–165, 2004.